Original Article

Mitigating the Oncogenic Roles of miR-629-5p and miR-660-5p Through Direct Binding by Two Potential Drug Targets for Colorectal Cancer Prevention

Fariborz Poorbaferani, Soheil Bolandi[1], Mohammad Abdolvand[2,3,4], Fatemeh Aghaie-Kheyrabadi[5], Nooshin Farhadian[4], Shirin Abdolvand[6], Fatemeh Maghool[7], Mohammad H. Emami[7], Alireza Fahim[7], Hojjatolah Rahimi[7], Elham Amjadi[7], Fatemeh D. N. Bon[8], Simin Hemati[9], Mansoor Salehi[2,3,4]

Department of Clinical Nutrition, School of Nutrition and Food Science, Food Security Research Center, Isfahan University of Medical Sciences, Isfahan, Iran, [1]Faculty of Medicine, Shiraz University of Medical Sciences, Shiraz, Iran, [2]Cellular, Molecular and Genetics Research Center, Isfahan University of Medical Sciences, Isfahan, Iran,

Address for correspondence:
Mr. Mohammad Abdolvand, Second Alley, Marefat Street, Valiasr Neighborhood, Postal Code: 8179685847, Isfahan City, Iran.
E-mail: m.abdolvand1366@gmail.com

Abstract

Background: Many studies have reported the oncogenic roles of microRNA (miRNA)-629-5p and miRNA-660-5p in various cancers. This study aimed to elucidate the oncogenic roles of miRNA-629-5p and miRNA-660-5p, focusing on their potential contributions to early colorectal cancer (CRC) detection. Additionally, this research examines the efficacy of Regorafenib and 3,3'-diindolylmethane (DIM) as therapeutic agents aimed at mitigating the oncogenic activities of these miRNAs by influencing their structural and conformational dynamics, thereby offering a preventive strategy against CRC. **Methods:** The study utilized quantitative real-time polymerase chain reaction (QRT-PCR) to confirm the overexpression of miR-629-5p and miR-660-5p in 40 CRC tissues compared to 40 standard samples and their association with clinicopathological factors. Molecular docking and molecular dynamics simulation were used to investigate Regorafenib and DIM binding modes to miR-629-5p and miR-660-5p. **Results:** QRT-PCR showed that miR-629-5p and miR-660-5p were overexpressed in CRC tissues. In silico molecular docking and dynamic simulation strengthened our hypothesis that Regorafenib and DIM were located in the structures of the mentioned miRNAs, resulting in a slight alteration in their structures during the interaction process. **Conclusions:** The study's findings suggest that miR-629-5p and miR-660-5p may have potential as predictive biomarkers and treatment targets for Preventing CRC and that Regorafenib and DIM may have miRNA binding properties. They indicated a high affinity to miRNA-629-5p compared with miRNA-660-5p created a slight change in its structure and can suppress its activity in CRC. However, extra experimental approaches are needed to approve our hypothesis.

Keywords: *3,3'-diindolylmethane (DIM), miR-629-5p, miR-660-5p, molecular docking, molecular dynamics simulation, regorafenib*

Introduction

CRC is a widely prevalent malignant condition and a primary contributor to global cancer-related deaths. In 2020, there were over 1.9 million newly reported CRC cases and 935,000 deaths across the world, representing 10% of total cancer cases and deaths.[1-4] Advances in the systemic treatment of CRC over the past two decades have been remarkable, primarily due to the utilization of chemotherapeutic drugs like fluoropyrimidines (FP) and innovative agents. These developments have substantially prolonged the central point for overall survival in metastatic CRC cases.[5-7]

As a therapeutic agent, Regorafenib [Figure 1a] is an orally administered multi-kinase inhibitor that adeptly suppresses the activity of angiogenic, stromal, and oncogenic protein kinases. Regorafenib has achieved approval for patients with heavily pre-treated metastatic CRC (mCRC) via the outcomes of a Phase III clinical trial, highlighting its overall survival (OS) benefit over best supportive care alone.[8] Previously, the standard approach to CRC treatment involved chemotherapy protocols featuring fluoropyrimidine, oxaliplatin, and irinotecan, along with targeted antiangiogenic drugs and anti-EGFR therapy for individuals with wild-type RAS tumors.[9] Former studies showed that Regorafenib has the potential to interact with oncogenic miRNAs to suppress CRC progression. For example, Chen *et al*.[6] demonstrated that Regorafenib interacts with miR-21 and changes its structure, leading to inhibiting its function

How to cite this article: Poorbaferani F, Bolandi S, Abdolvand M, Aghaie-Kheyrabadi F, Farhadian N, Abdolvand S, *et al*. Mitigating the oncogenic roles of miR-629-5p and miR-660-5p through direct binding by two potential drug targets for colorectal cancer prevention. Int J Prev Med 2025;16:33.

Access this article online

Website: www.ijpvmjournal.net/www.ijpm.ir

DOI: 10.4103/ijpvm.ijpvm_277_24

Quick Response Code:

[3]*Medical Genetics Research Center of Genome, Isfahan University of Medical Sciences, Isfahan, Iran,* [4]*Department of Genetics and Molecular Biology, School of Medicine, Isfahan University of Medical Science, Isfahan, Iran,* [5]*Department of Biology, Faculty of Science, Shahrekord University, Shahrekord, Iran,* [6]*Department of Genetics, Faculty of Sciences, Islamic Azad University, Shahrekord Branch, Shahrekord, Iran,* [7]*Poursina Hakim Digestive Diseases Research Center, Isfahan University of Medical Sciences, Isfahan, Iran,* [8]*Department of Cellular and Molecular Biology, Payam-e-Noor University of Mahmudabad, Mazandaran, Iran,* [9]*Department of Radiooncology, School of Medicine, Isfahan University of Medical Sciences, Isfahan, Iran*

First authors: *Fariborz Poorbaferani and Soheil Bolandi contributed equally as the first authors.*

in CRC. Thus, Regorafenib's features in CRC prevention by close interaction with oncogenic miRNAs made it a good candidate for evaluation in our study.

3,3'-diindolylmethane (DIM), represented in Figure 1b, is a chemical obtained from cruciferous greens and has displayed antitumor function in various types of human cancers, such as pancreatic and prostate cancer.[10,11] Blocking the WW Domain Containing E3 Ubiquitin Protein Ligase 1 (*WWP1)* and activating the tumor suppressor Phosphatase and tensin homolog (*PTEN*) while decreasing *PI3K-AKT-mTOR* signaling, may provide a valuable strategy for preventing and treating CRC.[12] According to Ye *et al*.'s[13] research, DIM may have potentially initiated apoptosis and autophagy in BGC-823 gastric cancer cells by influencing store-operated Ca^{2+} entry (*SOCE*) via the Ca^{2+}/AMPK/ER stress signaling pathway. In addition, DIM illustrated that it has the potential to bind with miR-21, which may alter the catalyzation process of dicer, an RNase III enzyme involved in miRNA transcription making it a good agent in target-based therapy.[14] We, therefore, selected DIM to investigate its ability to suppress both oncogenic miRNAs in this research, finding a new drug for cancer therapy.

Non-coding RNAs, especially miRNAs, regulate the expression of target mRNAs and contribute to the development of various cancer types.[15-17] MiRNAs with oncogenic features, like miR-629-5p and miR-660-5p, are critical players in various signaling cascades.[18-22] They are often found to be elevated in multiple cancer forms, with the majority of their documented targets being tumor suppressor genes.[22-24] For instance, miR-629-5p increased cell proliferation, and migration and acted as a tumor enhancer by suppressing CXXC finger protein 4 (CXXC4) a tumor suppressor gene in CRC.[18] In addition, overexpression of miR-660-5p resulted in the proliferation, invasion, and migration in non-small cell lung cancer (NSCLC) via targeting Krüppel-like factors-9 (KLF9) pathway while knockdown of it had a reverse effect.[25] The effective downregulation of two miRNAs linked to cancer growth suggests their potential as diagnostic markers and therapy targets for CRC.[21,26]

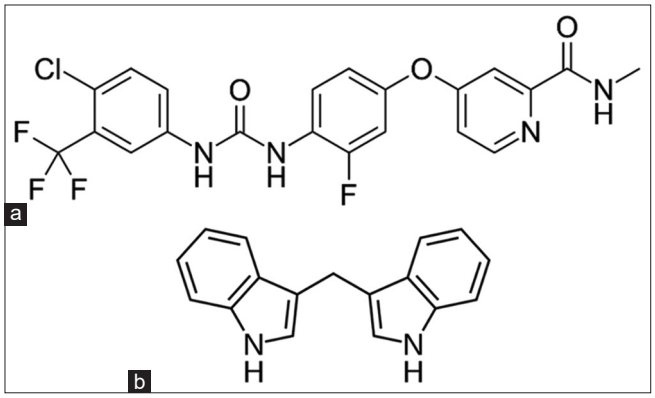

Figure 1: (a), (b). The Regorafenib and DIM structures

This study aimed to clarify the carcinogenic roles of miR-629-5p and miR-660-5p in CRC and evaluated how Regorafenib and DIM modulate these miRNAs to suppress their oncogenic functions. By targeting these molecular mechanisms, the research highlights potential strategies for the prevention and treatment of CRC. There is no study about the intermolecular association between Regorafenib and DIM with miR-629-5p and miR-660-5p. Thus, this is the first study to investigate the binding behavior of the related drugs with both miRNAs, utilizing several computational approaches to determine the affinity of these agents to miRNAs, the binding mode, and the conformational change of miRNAs after associating agents. Additionally, the binding position of the medications mentioned above within miRNAs was ascertained by dock-based blind docking calculations. The molecular mechanism and biological activity of DIM and Regorafenib, as well as the prognostic and therapeutic functions of miR-660-5p and miR-629-5p in colorectal cancer, can all be better understood with the aid of these investigations.

Materials and Methods

Materials

In this research, TRIzol reagent (Invitrogen Life Sciences, Carlsbad, California, Code Number: 15596026) was used for RNA extraction, Transcriptor First Strand cDNA Synthesis Kit (BioGenius, Korea, Code Number: 400203301) for complementary DNA (cDNA) synthesis and BioFact™ 2X Real-Time PCR Master Mix (Cat. Number: DQ383-40h) for quantitative real-time polymerase chain reaction (QRT-PCR) purpose was applied.

Methods

Molecular docking

Molecular docking through an established three-dimensional structure is an essential tool.[27,28] Using Auto dock 4.2.6 software, the molecular docking method for the miRNA with and without DIM and regorafenib as a ligand was used.[29,30] The RCSB-PDB (http://www.rcsb.org/pdb)[31] and

PubChem sites, respectively, provided the miRNA's 3D structure with PDB ID 3PEP and DIM and regorafenib.[32] Chimera UCSF software was used to optimize the structures that were produced, and the crystal structures were then stored in PDB format. The initial docking was done to find the precise spot where the ligand-binding occurred on the enzyme. To ascertain the optimal stereochemical and interaction mood of the DIM and regorafenib and miRNA configuration, final docking was performed.[33,34] The protein was stiff during the molecular docking process, whereas the DIM and regorafenib were completely flexible. For ligands, some elements were taken into consideration, such as orientations and random torsions. The ligand with the lowest binding energy was chosen to assess the kind of binding. The miRNA-DIM and regorafenib mixture's grid box size in the molecular docking studies was established at 80 Å × 80 Å × 80 Å. All of the essential hydrogen atoms were attached to the enzyme in the grid box with a grid spacing of 1 Å. The interval between grid points was 0.375 Å for all trials. For molecular docking investigations, a 100-run Lamarckian genetic method was used. Intermolecular interactions between DIM, regorafenib, and miRNA were surveyed using Chimera and R-studio discovery program version V 16.1.[35-39]

Dynamics simulation approaches

The Gromacs 2022.6 program was used to analyze the trajectory of the molecular dynamics (MD) simulation.[40-42] Protein ions and water molecules were counted using Amber 99sb's force field parameters.[43,44] miRNA-629 was positioned at the center of a cubic box containing 8209 water molecules to establish a neutral system. Following the addition of water molecules (TIP3P model) to the box, miRNA was positioned at the box's center, at a distance of 1 Å. To maintain charge neutrality, 44 Na+ ions and 24 Cl- ions were added to the box, which had dimensions of 6.39193 nm × 6.39193 nm × 6.39193 nm. In a similar fashion, miRNA-660 coexisted with 10,050 water molecules in the simulation box, along with 50 Na+ ions and 24 Cl- ions. The central box had dimensions of 6.81790 nm × 6.81790 nm × 6.81790 nm, employing the TIP3P water model. For the MD simulation, the compound with the lowest binding energy in the docking process between miRNAs and DIM and regorafenib was selected as the starting compound. The pressure within the simulation box was set to a reference pressure of 1 bar with a relaxation time of two femtoseconds. Energy minimization for DIM and regorafenib was carried out using the chimera ucsf and amber 99 algorithms. The MD simulation duration was set to 200 ns. Equilibration during the MD simulation occurred in two phases. The NVT and NPT ensembles were utilized during the MD simulation of the enzyme. The initial phase was conducted under an NVT ensemble (constant number of particles, volume, and temperature) to stabilize the system temperature. Pressure equilibration was carried out under an NPT ensemble where the number of particles, pressure, and temperature remained constant. NPT was employed during equilibration just before transitioning to a constant volume ensemble.[45] The LINCS algorithm constrained all bond lengths, while the Particle Mesh Ewald (PME) summation scheme was employed to calculate electrostatic interactions.[46,47] The system temperature was maintained at 310 K, with Lennard-Jones potential used to compute van der Waals interactions. Finally, parameters such as Rg, RMSF, and RMSD were analyzed.[40,41,43,46,48]

Patients and tissue specimens

This research acquired tissue specimens from 40 individuals diagnosed with CRC and 40 corresponding non-malignant tissues (totaling 80 samples). The specimens were gathered at the Poursina Hakim Center for Gastrointestinal Disease Research, Alzahra Hospital, Kashani, Amin, and Askariye Hospitals between 2018 and 2020, and all cases provided documented consent. None of the individuals had undergone surgical procedures, radiotherapy, or chemotherapy, and all tissue samples were reevaluated by a pathologist following the guidelines of the World Health Organization (WHO) classification. The tissues were processed and rendered anonymous by ethical and legal norms.

RNA extraction and QRT-PCR analysis

Total RNA was isolated from the specimens using the TRIzol reagent, and cDNA was produced from the obtained RNA using the Transcriptor First Strand cDNA Synthesis Kit The derived cDNA was then analyzed through QRT-PCR using the BioFact™ 2X Real-Time PCR Master Mix and the 7300 Real-Time PCR System (from Applied Biosystems). We used the Rotor-Gene 6000 system, with the following conditions: (a) 95°C for 15 min; (b) 40 cycles of 95°C for 20 s and 60°C for 30 s; and (c) 72°C for 30 s. The sequence of the primer for has-miR-629-5p was Forward 5'-GAGTTTTGGG TTTACGTTGGGA-3' and Reverse 5' GTCGTATCCAGTGCAGGG TCCGAGGTATTCGCACTGG ATACGACAGTTCT-3'. miR-660 primer sequences were as follows: Forward, 5'-GCCCGCTACCCAT TGCATATCG-3', and Reverse 5'-GTGCAGGGT CCGAGGT-3'. To assess the relative expression levels of miR-629-5p and miR-660-5p, the 2-ΔΔCt technique was employed, with GAPDH serving as an internal reference for normalization. For accuracy assurance, each tissue sample underwent triple analysis. The computation of 2-ΔΔCt utilizes the 2-CT values to indicate the relative expression levels of the target miRNAs.

Statistical analysis

The GraphPad Prism 9 tool was utilized for conducting statistical analyses. Various statistical assessments were applied to explore distinctions in miR-629-5p and miR-660-5p expression levels between CRC cases and the reference group. Additionally, correlations between RNA expression and clinical characteristics were

investigated. These examinations included both parametric and non-parametric t-tests, the signed-rank analysis, the Mann-Whitney test, and the Wilcoxon matched pairs analysis. Statistical significance was defined as results with a *P* value less than 0.05. To ensure the reliability of the findings, all assessments were carried out in both directions

Results and Discussion

miRNA-629-5p and miRNA-660-5p were upregulated in CRC tissues

This investigation identified miRNA-629-5p and miRNA-660-5p as prospective miRNAs for upcoming exploration. In this context, various rationales support this choice. As an example, these miRNAs play vital regulatory functions in diverse cancer signal routes, including the PI3K/AKT/mTOR signaling pathways, based on prior investigations. Moreover, contemporary research has indicated that the control of these miRNAs is disturbed in different malignancies, including breast, non-small cell lung carcinoma (NSCLC), colorectal, and ovarian tumors, potentially influencing the epithelial-mesenchymal transition (EMT) of malignant cells, in addition to their movement and infiltration [Table 1]. Investigating the expression of the aforementioned miRNAs, QRT-PCR revealed their increased levels in tumor tissues compared to those in standard samples. For instance, miR-629-5p (95% confidence interval [CI], -1.905 to -0.5066; $P < 0.0012$) exhibited a (log2 Fold Change=2.3) [Figure 2a]. Based on our findings, a favorable association between elevated miR-629-5p expression in tumor tissues and male malignancies was identified ($P < 0.0006$). Following adjustments for stage, location, age, and differentiation, it was revealed in the multivariable analysis that there was no substantial connection between the clinicopathological factors referenced and miR-629-5p expression [Table 2]. Regularly, Lu and colleagues reported that the role of miR-629-5p as a tumor-promoting gene is to stimulate growth and mobility while inhibiting cell death and medication responsiveness. Drawing from these discoveries, it can be deduced that miR-629-5p might function as a potential biomarker and therapeutic objective for individuals with colorectal carcinoma.[18] Consistently,

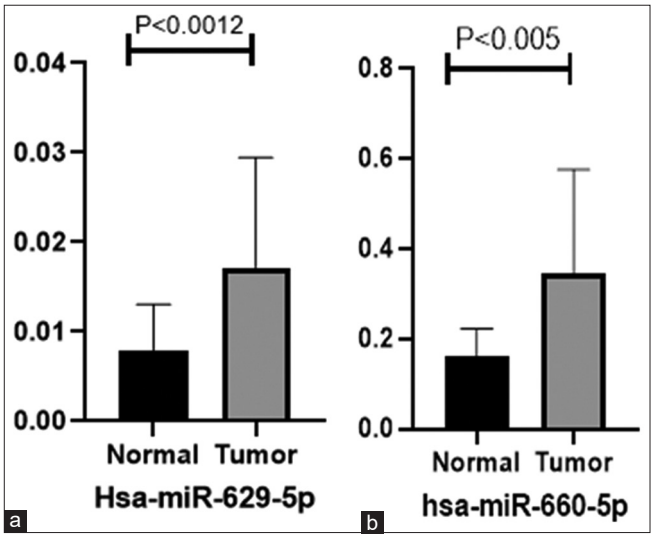

Figure 2: (a) and (b) show aberrant expression levels of has-miR-629-5p and has-miR-660-5p in tumor tissues compared to normal samples assessed by qPCR, respectively

Table 1: An overview of the role of miR-629-5p and miR-660-5p in different cancers

Author	Year	miR-629-5p function
Liu *et al*.[51]	2021	In the serum samples of NSCLC patients, it was positively regulated. Poor clinical outcomes of non-small cell lung cancer were linked to elevated serum levels of miR-629. miR-629 may serve as a promising new biomarker for NSCLC
Lu *et al*.[18]	2018	It was controlled in colon cancer cell lines and tissues. By directly regulating CXXC4, it suppresses apoptosis and 5-FU sensitivity in the evolution of CRC and acts as a tumor promoter by enhancing migration and proliferation.
Gao *et al*.[52]	2021	Osteosarcoma proliferation and migration were promoted by overexpression of CAV1 mRNA in osteosarcoma tissues and cells, as well as by directly targeting the mRNA.
Liu *et al*.[19]	2021	elevated in PCa tissues and an anchor protein A-kinase 13 direct target (AKAP13). It provides a new perspective on the intricate diagnosis and treatment of PCa.
Shao *et al*.[53]	2022	Inhibition of miR-629 may be a potential treatment target for ovarian cancer (OC), because overexpression can promote the growth, invasion, and migration of ovarian cancer (OC) by directly reducing TSPYL5 expression.
Peng *et al*.[20]	2020	Through the control of TET2 and PI3K/AKT/mTOR signaling, it regulated the advancement of breast cancer (BC).
Shen *et al*.[23]	2017	TFCP2 was an immediate downstream target of miR-660-5p and was upregulated in breast cancer cell lines. TFCP2 expression was inhibited by aberrant miR-660-5p expression. Human breast cancer cell migration, invasion, and proliferation can all be controlled by miR-660-5p.
Krishnan *et al*.[50]	2015	It is overexpressed in cases of breast cancer and can be a useful prognostic marker.
Wu *et al*.[22]	2020	It is upregulated in hepatocellular carcinoma (HCC) and can dramatically boost the rate of HCC cell division, clone creation, invasion, migration, and tumorigenic potential. It has been established that YWHAH targets the miR-660-5p and miR-660-5p/YWHAH axis, activating the PI3K/AKT pathway that supports EMT and cell cycle activities.

Table 2: Correlation between expression of has-miR-629-5p in CRC with the clinicopathologic feature

Clinicopathological parameters	Number of cases	Has-miR-629-5p		*P*
		Low	High	
Total	40	16	24	0.0012
Age (years)				0.4542
≤60	9	4	5	
>60	31	11	19	
Gender				
Female	20	9	11	0.1321
Male	20	7	13	
Location				0.9483
Colon	28	12	16	
Rectum	12	4	8	
Differentiation				0.7014
Well/moderately	32	22	18	
Poorly	8	2	6	
TNM stage				0.653
I–II	22	11	11	
III–IV	18	5	13	

Dr. Liu showed that miR-629-5p caused cell proliferation and migration in prostate cancer by directly targeting A-kinase Anchor Protein 13 (AKAP13) pathway. This study presented miR-629-5p as a new biomarker for clinical diagnosis and treatment.[49] Furthermore, QRT PCR unveiled that miR-660-5p exhibited higher expression levels in tumor tissues than their respective normal tissues ($P < 0.005$ and log2 fold change = 4.2) [Figure 2b]. Our findings suggest a favorable connection between the miR-660-5p expression and the susceptibility to CRC in males ($P < 0.0148$). Our investigation did not uncover any notable link between elevated miR-660-5p levels and various clinical attributes in CRC. As noted by Krishnan and colleagues, the excessive expression of miR-660-5p in breast cancer suggests its potential use as a dependable prognostic indicator.[50] Similarly, Pan and his group showed that miR-660-5p was upregulated in liver cancer (LC) tissues, resulting in LC proliferation by targeting regulatory subunit βα (PPP2R2A) expression.

Hence, the increased expression of both miR-629-5p and miR-660-5p could be seen as possible indicators for the early identification of CRC, especially in both male and female individuals. Nonetheless, additional research is essential to validate these results and assess the precision and effectiveness of miR-629-5p and miR-660-5p as early detection biomarkers for CRC.

Modeling and analysis of regorafenib and DIM interaction with miR-629-5p and miR-660-5p

Molecular docking involves a computational methodology that utilizes algorithms to anticipate the attachment affinity of a ligand to a receptor and its associated binding manner within a designated active region. This method can offer valuable perspectives into the bonding mechanism of minor compounds and aid in developing novel pharmaceutical prospects. Through estimating the connections between a ligand and its receptor, molecular docking can aid in the recognition of potential drugs and the enhancement of their attachment characteristics.[47] For this research, molecular docking was performed to explore the molecular interactions between Regorafenib and DIM with miR-629-5p and miR-660-5p. Figure 3a-h displays the best docking position and 2D conformational interactions of ligands with miRNAs. The findings indicated that hydrogen bonds were crucial in establishing complexes between Regorafenib, Diindolylmethane, and miR-629-5p and miR-660-5p. DIM established five conventional hydrogen bonds with G13, G14, G10, U11, and C9 nucleotides within miR-629-5p [Figure 3a] and interacted with U7 and C9 nucleotides in miR-660-5p [Figure 3c]. Figure 3e depicts Regorafenib creating five conventional hydrogen bonds with G15, A16, G10, U12, and C9 nucleotides while residing at the center of the loop within miR-629-5p, thereby connecting two strands. Regorafenib ultimately interacted with G16, A18, and G19 nucleotides within the loop conformation of miR-660-5p, as illustrated in Figure 3g. The outcomes of this assessment can be observed in Table 3. Per the docking analysis, the strong binding affinity was established for Regorafenib with miR-629-5p (-7.61 kcal/mol), followed by the Regorafenib-miR-660-5p (-6.29 kcal/mol), Diindolylmethane-miR-629-5p (-6.12 kcal/mol), and Diindolylmethane-miR-660-5p (-4.4 kcal/mol).

Molecular dynamic simulation

A molecular dynamics (MD) simulation was carried out to explore the structural steadiness and alterations in the conformation of miR-629 and miR-660 following their interaction with DIM and Regorafenib. The Root Mean Square Deviation (RMSD) serves as a valuable metric for assessing the structural stability of biomolecules when bound to a ligand across a period.[54] During a 200 ns molecular dynamics simulation, RMSD measurements were taken for the atoms in miRNA-629 and miRNA-660, along with their corresponding ligand-miRNA complexes, compared to their initial configurations. During the simulation study, the PDB structure of miRNAs and the binding structures of DIM and Regorafenib with the protein that scored the highest were used as reference structures. Figure 4a and b and Table 4 display the RMSD values of natural miRNAs and complexes. According to Table 4 and Figure 4a, the mean RMSD for free miR-629-5p was 0.866 ± 0.050 nm, whereas that of regorafenib-miRNA-629-5p was 0.726 ± 0.036. This suggests that regorafenib and miRNA-629-5p have a safe interaction, which promotes the stability of miRNA-629-5p. Also, the average RMSD of the Diindolylmethane-miRNA-629-5p complex (0.618 ± 0.030) was considerably lower than that of free miRNA-629-5p, suggesting that miRNA-629 is more stable when attached to Diindolylmethane. The average RMSD

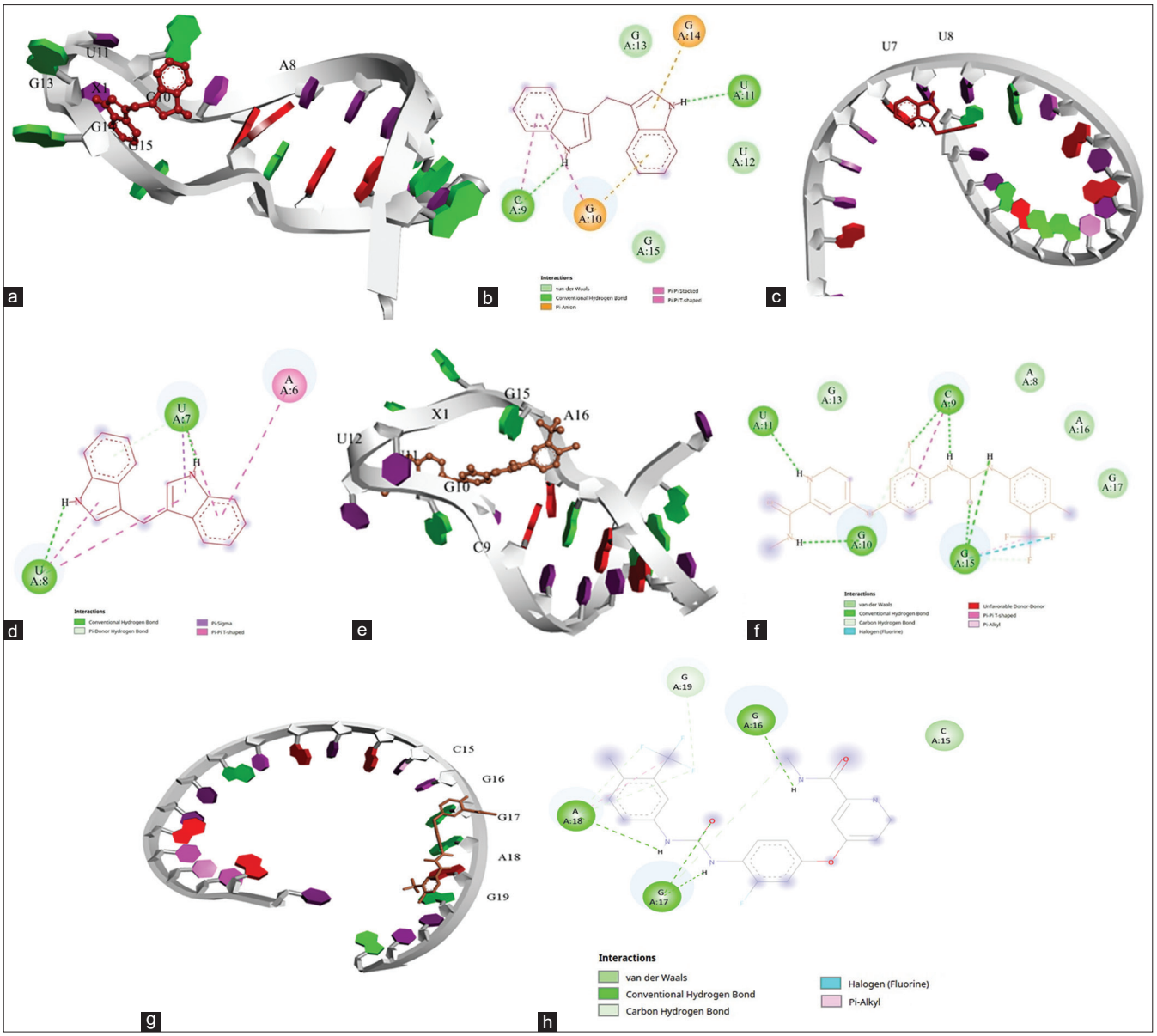

Figure 3: Nonbonding interactions of (a) DIM-mir-629-5p (interaction with G13, G14, G10, U11 and C9 nucleotide), (b) 2D conformation interaction of DIM-mir-629-5p, (c) DIM-mir-660-5p (interaction with U7 and C9 nucleotide), (d) 2D conformation interaction of DIM-mir-660-5p, (e) Regorafenib-mir-629-5p (interaction with G16, A18, and G19 nucleotide), (f) 2D conformation interaction of Regorafenib-mir-629-5p, (g) Regorafenib-mir-660 (interaction with G15, A16, G10, U12 and C9 nucleotide), (h) 2D conformation interaction of Regorafenib-mir-629-5p, pose predicted by AutoDock and visualized by Discovery studio visualizer

Table 3: Docking results in the form of binding affinity of DIM and used for in silico screening against miRNA-629-5p and miRNA-660-5p (AutoDock scores are in kcal.mol^{-1})

Receptor/ Protein	Ligand-receptor	BE* kcal.mol^{-1}	FIE** kcal. mol^{-1}	EIC*** μM. mM^{-1}	Estimated Inhibition Constant, Ki (micromolar)
miRNA-629	Diindolylmethane	-6.12	-6.72	-0.04	32.59
	Regorafenib	-7.61	-9.40	-0.42	2.63
miRNA-660	Diindolylmethane	-4.40	-5.00	-0.02	593.47
	Regorafenib	-6.29	-8.08	-0.47	24.66

values for the Diindolylmethane-miRNA-660 and Regorafenib-miRNA-660 complexes were 1.397 ± 0.036 and 1.594 ± 0.043, respectively, as shown in Table 4, which is greater than the corresponding value for the free miRNA-660-5p (1.259 ± 0.018). To put it another way, the RMSD value increased for both complexes, but more so for Regorafenib-miRNA-660 than for Diindolylmethane-miRNA-660-5p [Figure 4b]. This can

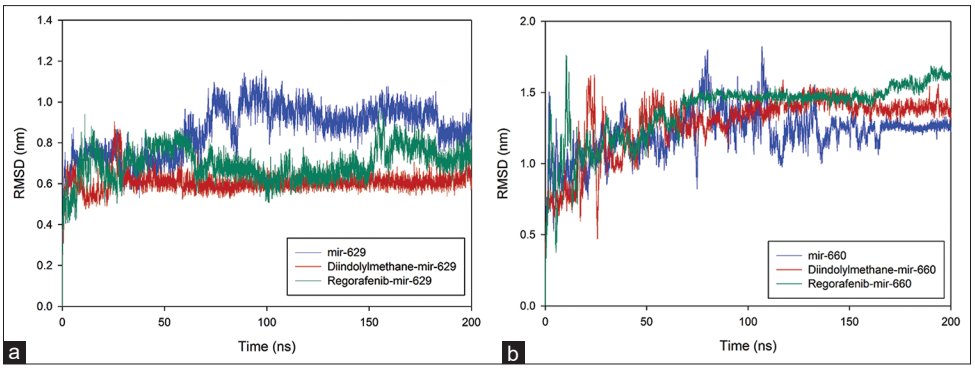

Figure 4: Changes in the Root Mean Square Deviation (RMSD) during simulation time. Plot a to the RMSD of miRNA-629 alone (blue line), DIM-miRNA-629(red line), and Regorafenib-miRNA-629 (green line). Plot b to the RMSD of miRNA-660 alone (blue line), DIM-miRNA-660 (red line), and Regorafenib-miRNA-660 (green line)

Table 4: Summary of simulation information in the form of mean±standard deviation

Name	RMSD (nm)	Rg (nm)	RMSF (nm)	H-bond between RNA-solvation (number)	H-bond between RNA-protein-protein (number)
miRNA-629	0.866±0.050	1.450±0.056	0.522±0.149	220.270±7.692	24.036±2.441
Diindolylmethane-miRNA-629	0.618±0.030	1.348±0.027	0.231±0.095	213.233±7.759	24.983±2.518
Regorafenib-miRNA-629	0.726±0.036	1.432±0.042	0.333±0.108	207.423±7.535	30.150±2.996
miRNA-660	1.259±0.018	1.264±0.031	0.767±0.217	211.444±7.698	32.040±2.687
Diindolylmethane-miRNA-660	1.397±0.036	1.281±0.026	0.723±0.200	218.620±8.210	23.326±2.837
Regorafenib-miRNA-660	1.594±0.043	1.192±0.034	0.575±0.197	213.079±9.846	28.969±4.897

be explained by the fact that miRNA was destabilized due to DIM and Regorafenib binding to miRNA-660-5p. Small RMSD values in a simulation are often taken to reflect a stable system state. This demonstrates that system stability results from DIM and Regorafenib safe binding to miR-629-5p. In contrast, these ligands binding to miR-660-5p cause system instability.

To assess variations in compaction and analyze the structural compactness of the miRNA macromolecules throughout the molecular dynamic simulation, the gyration radius (Rg) was measured. The protein's radius of gyration represents the root-mean-square distance of all atoms from the center of gravity, providing insights into the interplay between protein compaction and folding. Additionally, to investigate changes in miRNA conformation and fluctuations in macromolecule structure, the gyration radius (Rg) was utilized.[55-57] The alterations in Rg for miRNA-629 and miRNA-660, as well as the impact of DIM and Regorafenib additions on the system, are depicted in Figure 5a and b. These observations shed light on the dynamic behavior and structural changes occurring within the system. Based on the data presented in Figure 5a, the mean Rg values for the DIM-miRNA-629-5p and Regorafenib-miRNA-629-5p complexes were approximately 1.348 ± 0.027 nm and 1.432 ± 0.042 nm, respectively, which were lower than the mean Rg of the free miRNA-629-5p system (1.450 ± 0.056 nm). These findings indicate an enhancement in the compaction of the miRNA-629-5p structure following the binding of both drugs to miRNA-629-5p. Figure 5b demonstrates that the other three systems also experienced changes in their Rg values. The average Rg values for the DIM-miRNA-660-5p and Regorafenib-miRNA-660-5p complexes were 1.281 ± 0.026 nm and 1.192 ± 0.034 nm, respectively. Referring to Table 4, the Rg value for DIM-miRNA-629-5p displayed a minimal increase compared to miRNA-629-5p (1.264 ± 0.031 nm), which is insignificant. However, for the Regorafenib-miRNA-629-5p complex, there was a decrease in Rg by 1.192 ± 0.034 nm, indicating a more closed structure and increased compression of the miRNA-629-5p macromolecule.

By computing the time-averaged RMSF values for free miRNA-629-5p, Regorafenib-miRNA-629-5p, and DIM-miRNA-629-5p complexes, we can assess the mobility of miRNA. As depicted in Figure 6a and Table 4, the RMSF values for residues in the DIM-miRNA-629-5p complex exhibited notable reductions compared to free miRNA-629-5p, indicating that binding to DIM resulted in decreased residue fluctuations. So, the flexibility of residues in the DIM-miRNA-629-5p complex (0.231 ± 0.095) was significantly reduced, indicating that the interaction between miRNA-629-5p and Diindolylmethane led to decreased residue flexibility. Comparatively, the mean RMSF value for free miRNA-629-5p was 0.522 ± 0.149 nm, while for the Regorafenib-miRNA-629-5p complex, it was 0.333 ± 0.108 nm [Table 4]. This suggests that the presence of both ligands reduced the flexibility of miRNA-629-5p.

In Figure 6b and Table 4, the RMSF values of individual residues in the Regorafenib-miRNA-660-5p

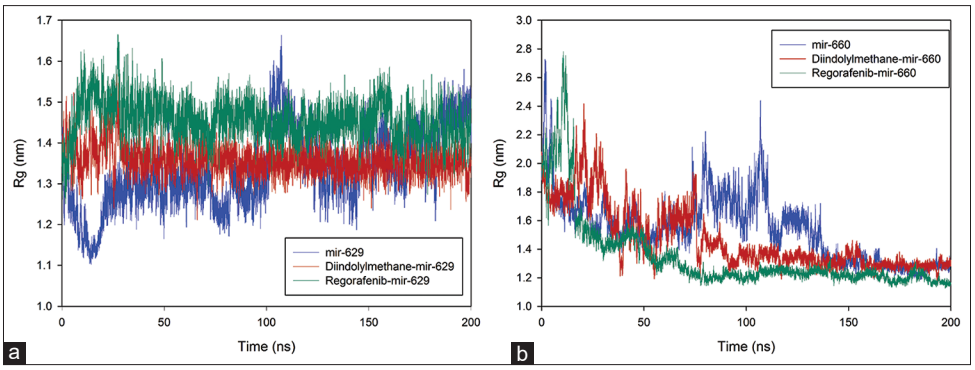

Figure 5: Changes in the Radius of gyration (Rg) during simulation time. Plot a to the Rg of miRNA-629 alone (blue line), Diindolylmethane-miRNA-629 (red line), and Regorafenib-miRNA-629 (green line). Plot b to the Rg of miRNA-660 alone (blue line), Diindolylmethane-miRNA-660 (red line), and Regorafenib-miRNA-660 (green line)

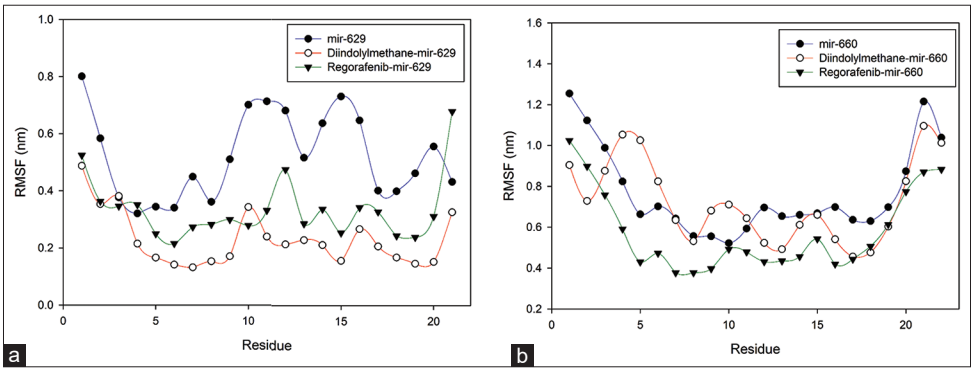

Figure 6: Changes in the Root-mean-square fluctuation (RMSF) during simulation time. Plot a to the RMDF of miRNA-629 alone (blue line), DIM-miRNA-629 (green line), and Regorafenib-miRNA-629 (red line). Plot b to the RMSF of miRNA-660 alone (blue line), DIM-miRNA-660 (red line), and Regorafenib-miRNA-660 (green line)

complex were reduced, resulting in an average RMSF value of 0.575 ± 0.197, compared to free miRNA-660-5p (0.767 ± 0.217). Similarly, the DIM-miRNA-660-5p complex exhibited a slight decrease in RMSF values for residues, with an average RMSF value of 0.723 ± 0.200, lower than that of free miRNA-660-5p. These findings emphasize that the interaction between miRNA-660-5p and the two ligands of dindolylmethane and regorafenib contributes to a reduction in residue flexibility. Furthermore, Table 4 presents the average number of hydrogen bonds between RNA and solvation for free miRNAs and the DIM and Regorafenib-miRNA complexes. The results indicate that a reduction in intermolecular H- bonds signifies a more compact structure of miRNA-629-5p when DIM and Regorafenib are present. This finding aligns with the Rg analysis; however, it is contrary for regorafenib-miRNA-660-5p.

Conclusions

Our study shows that miRNA-629-5p and miR-660-5p are overexpressed and could be promising targets for prognostic and therapeutic purposes in CRC, especially in male CRC tumors. However, additional experimental studies are necessary to comprehend the primary mechanism of these miRNAs in CRC. Additionally, molecular dynamic simulation and docking provide insight into the binding site and changes in stability and conformation of miR-629-5p and miR-660-5p. According to the molecular docking data, DIM and Regorafenib both strongly bind to the miRNAs, and the RMSD, Rg, and RMSF values indicate that miR-629-5p is less stable and compact than miR-660-5p in the presence of these compounds. Hydrogen bonding is the dominant force driving the complex formation between the miRNAs and their respective ligands. These findings suggest that DIM and Regorafenib may be able to inhibit miRNA-629-5p's oncogenic role, preventing CRC. These results enhance our understanding of the interaction mechanism between DIM and Regorafenib with miR-629-5p and miR-660-5p, thereby advancing research on these drugs' ability to inhibit related miRNAs.

Abbreviations

CRC	*Colorectal Cancer*
miRNAs	*microRNAs*
DIM	3,3'-diindolylmethane
QRT-PCR	Quantitative Real-Time Polymerase Chain Reaction
FP	Fluoropyrimidines
OS	Overall Survival
EMT	Epithelial-Mesenchymal Transition

NSCLC	Non-Small Cell Lung Carcinoma
RMSD	Root Mean Square Deviation
Rg	Gyration radius

Acknowledgments

We highly appreciate the Shahrekord University, Iran, for assisting in this investigation.

Financial support and sponsorship

Isfahan University of Medical Sciences was responsible for the financial support and the Poursina Hakim Gastrointestinal Disease Research Center provided the CRC tissues

Conflicts of interest

There are no conflicts of interest.

Received: 09 Sep 24 **Accepted:** 02 Dec 24
Published: 28 May 25

References

1. Wang X, Cheng H, Zhao J, Li J, Chen Y, Cui K, *et al*. Long noncoding RNA DLGAP1-AS2 promotes tumorigenesis and metastasis by regulating the Trim21/ELOA/LHPP axis in colorectal cancer. Mol Cancer 2022;21:1-19. doi: 10.1186/s12943-022-01675-w.
2. Karimi Z, Moghaddam NA, Yousefi M, Abdolvand M, Zamani A, Dolatabadi NF, *et al*. Dysregulated of the FAM138E and CLRN1-AS1 lncRNAs could be diagnosis biomarkers in colorectal cancer. Hum Gene 2024;39:201249. doi: 10.1016/j.humgen.2023.201249.
3. Maimard Y, Woradet S, Chaimay B. Factors associated with mortality among patients with colorectal cancer at the secondary care hospital in Southern Thailand: Hospital-based retrospective cohort study. Int J Prev Med 2023;14:13.
4. Eshaghi F, Fakhar HBZ, Ghane M, Shokry J. Diagnostic evaluation of streptococcus gallolyticus infection in patients with colon diseases by polymerase chain reaction (PCR) and culturing methods. Int J Cancer Manag 2020;13:e101903. doi: 10.5812/ijcm.101903.
5. Källberg J, Harrison A, March V, Bērziņa S, Nemazanyy I, Kepp O, *et al*. Intratumor heterogeneity and cell secretome promote chemotherapy resistance and progression of colorectal cancer. Cell Death Dis 2023;14:306.
6. Chen X, Xie B, Cao L, Zhu F, Chen B, Lv H, *et al*. Direct binding of microRNA-21 pre-element with Regorafenib: An alternative mechanism for anti-colorectal cancer chemotherapy? J Mol Graphics Model 2017;73:48-53.
7. Harchegani HB, Moghaddasi H. Designing a hybrid method of artificial neural network and particle swarm optimization to diagnosis polyps from colorectal CT images. Int J Prev Med 2024;15:4.
8. Loupakis F, Antonuzzo L, Bachet J-B, Kuan F-C, Macarulla T, Pietrantonio F, *et al*. Practical considerations in the use of regorafenib in metastatic colorectal cancer. Ther Adv Med Oncol 2020;12:1758835920956862. doi: 10.1177/1758835920956862.
9. Novakova-Jiresova A, Kopeckova K, Boublikova L, Chloupkova R, Melichar B, Petruzelka L, *et al*. Regorafenib for metastatic colorectal cancer: An analysis of a registry-based cohort of 555 patients. Cancer Manag Res 2020;12:5365-72.
10. Gao X, Liu J, Cho KB, Kedika S, Guo B. Chemopreventive agent 3, 3′-Diindolylmethane inhibits MDM2 in colorectal cancer cells. Int J Mol Sci 2020;21:4642. doi: 10.3390/ijms21134642.
11. Thomson CA, Ho E, Strom MB. Chemopreventive properties of 3, 3′-diindolylmethane in breast cancer: Evidence from experimental and human studies. Nutr Rev 2016;74:432-43.
12. Jiang Y, Fang Y, Ye Y, Xu X, Wang B, Gu J, *et al*. Anti-cancer effects of 3, 3'-diindolylmethane on human hepatocellular carcinoma cells is enhanced by calcium ionophore: The role of cytosolic ca2+and p38 mapK. Front Pharmacol 2019;10:1167. doi: 10.3389/fphar. 2019.01167.
13. Ye Y, Li X, Wang Z, Ye F, Xu W, Lu R, *et al*. 3, 3'-Diindolylmethane induces gastric cancer cells death via STIM1 mediated store-operated calcium entry. Int J Biol Sci 2021;17:1217.
14. Junaid M, Dash R, Islam N, Chowdhury J, Alam MJ, Nath SD, *et al*. Molecular simulation studies of 3, 3′-diindolylmethane as a potent MicroRNA-21 antagonist. J Pharm Bioallied Sci 2017;9:259-65.
15. Abdolvand M, Sadeghi M, Emami MH, Fahim A, Rahimi H, Amjadi E, *et al*. Constructing a novel competing Endogenous RNAs network based on NR3C1 and X-linked inhibitor of apoptosis protein genes reveals potential prognostic biomarkers in colorectal cancer. J Res Med Sci 2022;27:71.
16. Asyura MMAZ, Komariah M, Amirah S, Faisal EG, Maulana S, Platini H, *et al*. Analysis of varying MicroRNAs as a novel biomarker for early diagnosis of preeclampsia: A scoping systematic review of the observational study. Int J Prev Med 2023;14:36.
17. Hosseini M, Sahebi R, Aghasizadeh M, Yazdi DF, Salaribaghoonabad R, Godsi A, *et al*. Investigating the predictive value of microRNA21 as a biomarker in induced myocardial infarction animal model. Gene Rep 2022;27:101578. doi: 10.1016/j.genrep. 2022.101578.
18. Lu J, Lu S, Li J, Yu Q, Liu L, Li Q. MiR-629-5p promotes colorectal cancer progression through targetting CXXC finger protein 4. Biosci Rep 2018;38:BSR20180613. doi: 10.1042/BSR20180613.
19. Liu Y, Zhao S, Wang J, Zhu Z, Luo L, Xiang Q, *et al*. MiR-629-5p promotes prostate cancer development and metastasis by targeting AKAP13. Front Oncol 2021;11:754353. doi: 10.3389/fonc. 2021.754353.
20. Peng B, Li C, He L, Tian M, Li X. miR-660-5p promotes breast cancer progression through down-regulating TET2 and activating PI3K/AKT/mTOR signaling. Braz J Med Biol Res 2020;53:e9740. doi: 10.1590/1414-431×20209740.
21. Nashtahosseini Z, Aghamaali MR, Sadeghi F, Heydari N, Parsian H. Circulating status of microRNAs 660-5p and 210-3p in breast cancer patients. J Gene Med 2021;23:e3320. doi: 10.1002/jgm. 3320.
22. Wu Y, Zhang Y, Wang F, Ni Q, Li M. MiR-660-5p promotes the progression of hepatocellular carcinoma by interaction with YWHAH via PI3K/Akt signaling pathway. Biochem Biophys Res Commun 2020;531:480-9.
23. Shen Y, Ye Y, Ruan L, Bao L, Wu M, Zhou Y. Inhibition of miR-660-5p expression suppresses tumor development and metastasis in human breast cancer. Genet Mol Res 2017;16:1-11. doi: 10.4238/gmr16019479.
24. Abdolvand M, Chermahini ZM, Bahaloo S, Emami MH, Fahim A, Rahimi H, *et al*. New long noncoding RNA biomarkers and ceRNA networks on miR-616-3p in colorectal cancer: Bioinformatics-based study. J Res Med Sci 2024;29:10.
25. Qi Y, Zha W, Zhang W. Exosomal miR-660-5p promotes tumor growth and metastasis in non-small cell lung cancer. J BUON 2019;24:599-607.
26. Shao L, Shen Z, Qian H, Zhou S, Chen Y. Knockdown of miR-629 inhibits ovarian cancer malignant behaviors by targeting testis-specific Y-like protein 5. DNA Cell Biol 2017;36:1108-16.

27. Kelly SM, Price NC. The use of circular dichroism in the investigation of protein structure and function. Curr Protein Pept Sci 2000;1:349-84.
28. Momeni L, Farhadian S, Shareghi B. Study on the interaction of ethylene glycol with trypsin: Binding ability, activity, and stability. J Mol Liq 2022;350:118542. doi: 10.1016/j.molliq.2022.118542.
29. Asemi-Esfahani Z, Shareghi B, Farhadian S, Momeni L. Food additive dye–lysozyme complexation: Determination of binding constants and binding sites by fluorescence spectroscopy and modeling methods. J Mol Liq 2022;363:119749. doi: 10.1016/j.molliq.2022.119749.
30. Yadollahi E, Shareghi B, Farhadian S. Noncovalent interactions between quinoline yellow and trypsin: *In vitro* and in silico methods. J Mol Liq 2022;353:118826. doi: 10.1016/j.molliq.2022.118826.
31. Yu J, Li X, Liu H, Peng Y, Wang X, Xu Y. Interaction behavior between five flavonoids and pepsin: Spectroscopic analysis and molecular docking. J Mol Struct 2021;1223:128978. doi: 10.1016/j.molstruc.2020.128978.
32. Yazdani F, Shareghi B, Farhadian S, Momeni L. Structural insights into the binding behavior of flavonoids naringenin with Human Serum Albumin. J Mol Liq 2022;349:118431. doi: 10.1016/j.molliq.2021.118431.
33. Farajzadeh-Dehkordi N, Farhadian S, Zahraei Z, Asgharzadeh S, Shareghi B, Shakerian B. Insights into the binding interaction of Reactive Yellow 145 with human serum albumin from a biophysics point of view. J Mol Liq. 2023;369:120800. doi: 10.1016/j.molliq. 2022.120800.
34. Dehdasht-Heidari N, Shareghi B, Farhadian S, Momeni L. Investigation on the interaction behavior between safranal and pepsin by spectral and MD simulation studies. J Mol Liq 2021;344:117903. doi: 10.1016/j.molliq.2021.117903
35. Hashemi-Shahraki F, Shareghi B, Farhadian S. Investigation of the interaction behavior between quercetin and pepsin by spectroscopy and MD simulation methods. Int J Biol Macromol 2023;227:1151-61.
36. Aghaie-Kheyrabadi F, Shareghi B, Farhadian S. Molecular interaction between cypermethrin and myoglobin: Spectroscopy and molecular dynamics simulation analysis. J Mol Liq 2024;395:123949. doi: 10.1016/j.molliq.2024.123949.
37. Berman HM, Westbrook J, Feng Z, Gilliland G, Bhat TN, Weissig H, *et al*. The protein data bank. Nucleic Acids Res 2000;28:235-42.
38. Wang Y, Suzek T, Zhang J, Wang J, He S, Cheng T, *et al*. PubChem bioassay: 2014 update. Nucleic Acids Res 2014;42:D1075-82.
39. Li Q, Cheng T, Wang Y, Bryant SH. PubChem as a public resource for drug discovery. Drug Discov Today 2010;15:1052-7.
40. Gholizadeh M, Shareghi B, Farhadian S. Elucidating binding mechanisms of naringenin by alpha-chymotrypsin: Insights into non-binding interactions and complex formation. Int J Biol Macromol 2023;253:126605. doi: 10.1016/j.ijbiomac.2023.126605.
41. Rawat R, Kant K, Kumar A, Bhati K, Verma SM. HeroMDAnalysis: An automagical tool for GROMACS-based molecular dynamics simulation analysis. Future Med Chem 2021;13:447-56.
42. Raeessi-Babaheydari E, Farhadian S, Shareghi B. Comparative studies on the interaction of ascorbic acid with gastric enzyme using multispectroscopic and docking methods. J Mol Struct 2021;1245:131270. doi: 10.1016/j.molstruc.2021.131270.
43. Yoo J. On the stability of protein–DNA complexes in molecular dynamics simulations using the CUFIX corrections. J Korean Phys Soc 2021;78:461-6.
44. Farajzadeh-Dehkordi M, Darzi S, Rahmani B, Farhadian S. A novel insight into the cytotoxic effects of Tephrosin with calf thymus DNA: Experimental and in silico approaches. J Mol Liq 2021;324:114728. doi: 10.1016/j.molliq.2020.114728.
45. Momeni L, Shareghi B, Saboury AA, Farhadian S. The effect of spermine on the structure, thermal stability and activity of bovine pancreatic trypsin. RSC Adv 2016;6:60633-42.
46. Essmann U, Perera L, Berkowitz ML, Darden T, Lee H, Pedersen LG. A smooth particle mesh Ewald method. J Chem Phys 1995;103:8577-93.
47. Dehkordi MF, Farhadian S, Abdolvand M, Soureshjani EH, Rahmani B, Darzi S. Deciphering the DNA-binding affinity, cytotoxicity and apoptosis induce as the anticancer mechanism of Bavachinin: An experimental and computational investigation. J Mol Liq 2021;341:117373. doi: 10.1016/j.molliq. 2021.117373.
48. Farhadian S, Shareghi B, Saboury AA, Evini M. The influence of putrescine on the structure, enzyme activity and stability of α-chymotrypsin. RSC Adv 2016;6:29264-78.
49. Liu Y, Zhao S, Wang J, Zhu Z, Luo L, Xiang Q, *et al*. MiR-629-5p promotes prostate cancer development and metastasis by targeting AKAP13. Front Oncol 2021;11:754353. doi: 10.3389/fonc.2021.754353.
50. Krishnan P, Ghosh S, Wang B, Li D, Narasimhan A, Berendt R, *et al*. Next generation sequencing profiling identifies miR-574-3p and miR-660-5p as potential novel prognostic markers for breast cancer. BMC Genomics 2015;16:1-17. doi: 10.1186/s12864-015-1899-0.
51. Liu F, Li T, Hu P, Dai L. Upregulation of serum miR-629 predicts poor prognosis for non-small-cell lung cancer. Dis Markers 2021;2021:8819934. doi: 10.1155/2021/8819934.
52. Gao C, Gao J, Zeng G, Yan H, Zheng J, Guo W. MicroRNA-629-5p promotes osteosarcoma proliferation and migration by targeting caveolin 1. Braz J Med Biol Res 2021;54:e10474. doi: 10.1590/1414-431X202010474.
53. Shao L, Shen Z, Qian H, Zhou S, Chen Y. Knockdown of miR-629 Inhibits Ovarian Cancer Malignant Behaviors by Targeting Testis-Specific Y-Like Protein 5 2017;36:1108-16.
54. Farhadian S, Shareghi B, Tirgir F, Reiisi S, Dehkordi NG, Momeni L, *et al*. Design, synthesis, and anti-gastric cancer activity of novel 2, 5-diketopiperazine. J Mol Liq 2019;294:111585. doi: 10.1016/j.molliq.2019.111585.
55. Ljung F, André I. ZEAL: Protein structure alignment based on shape similarity. Bioinformatics 2021;37:2874-81.
56. Aghaie-Kheyrabadi F, Shareghi B, Farhadian S. Molecular insights into the interaction between myoglobin and Imidacloprid: Multi-spectral experiments and computational simulations. J Mol Liq 2024:124341. doi: 10.1016/j.molliq. 2024.124341.
57. Rohani F, Hosseini SHK, Hosseini D, Bahaloo S, Ghiabi S, Soureshjani EH, *et al*. The effect of novel 3R, 6R-bis (4-hydroxy benzyl) piperazine-2, 5-dione (BHBPPD) derivatives on the expression of caspases in gastric cancer: A molecular docking and dynamics simulation. Arab J Chem 2023;16:105260. doi: 10.1016/j.arabjc.2023.105260.